World Academy of Science, Engineering and Technology
International Journal of Geological and Environmental Engineering
Vol:8, No:2, 2014

Factors Affecting the Ultimate Compressive Strength of the Quaternary Calcarenites, North Western Desert, Egypt

M. A. Rashed, A. S. Mansour, H. Faris, W. Afify

Abstract**—**The calcarenites carbonate rocks of the Quaternary ridges, which extend along the northwestern Mediterranean coastal plain of Egypt, represent an excellent model for the transformation of loose sediments to real sedimentary rocks by the different stages of meteoric diagenesis. The depositional and diagenetic fabrics of the rocks, in addition to the strata orientation, highly affect their ultimate compressive strength and other geotechnical properties.

There is a marked increase in the compressive strength (UCS) from the first to the fourth ridge rock samples. The lowest values are related to the loose packing, weakly cemented aragonitic ooid sediments with high porosity, besides the irregularly distributed of cement, which result in decreasing the ability of these rocks to withstand crushing under direct pressure. The high (UCS) values are attributed to the low porosity, the presence of micritic cement, the reduction in grain size and the occurrence of micritization and calcretization processes.

The strata orientation has a notable effect on the measured (UCS). The lowest values have been recorded for the samples cored in the inclined direction; whereas the highest values have been noticed in most samples cored in the vertical and parallel directions to bedding plane. In case of the inclined direction, the bedding planes were oriented close to the plane of maximum shear stress. The lowest and highest anisotropy values have been recorded for the first and the third ridges rock samples, respectively, which may attributed to the relatively homogeneity and well sorted grainstone of the first ridge rock samples, and relatively heterogeneity in grain and pore size distribution and degree of cementation of the third ridge rock samples, besides, the abundance of shell fragments with intraparticle pore spaces, which may produce lines of weakness within the rock.

Keywords**—**Compressive strength, Anisotropy, Calcarenites, Egypt.

I. Introduction

THE northwestern Mediterranean coastal plain of Egypt is considered one of the most important areas in Egypt suitable for tourism, industrial, and agricultural activities. It is characterized by a series of at least eight elongated parallel Quaternary beach limestone ridges; extend along the Mediterranean coast [1], [2]. The carbonate rocks of these ridges are quarried to use as building stones for many tourist sites and summer resorts along the Mediterranean coast or as raw materials for chemical and cement industries. Additionally, these rocks are considered as sites for shallow subsurface water aquifers.

The sediments of these ridges are subjected to different meteoric diagenetic processes including: cementation, dissolution, recrystallization, micritization and partial compaction. The degree of diagenesis varies as a function of the original sediments mineralogy, texture, porosity, permeability, hydrological regime and time. These factors highly affect the petrophysical and geotechnical properties of these porous calcarenite carbonate rocks.

Most of the preceding works dealt with the origin, mode of formation, depositional environment and diagenetic history of the calcarenite carbonate ridges [1]-[9]. Few studies have been conducted to describe the geotechnical characteristics of these rocks [10]-[12]. The present study aims to: 1) describe, petrographically, these calcarenite carbonate rocks and measure some geotechnical properties in the three directions (vertical, inclined, and parallel to the bedding plane) in order to study the anisotropism of these properties, 2) discus the factors controlling the engineering behavior of these rocks with attention to their compressive strength and give their engineering classification, and 3) determine the mutual relationships between the different geotechnical parameters in the form of empirical equations. The present work focuses on studying the most northern four ridges at Burg El-Arab area (Fig. 1). These four ridges are named from the most seaward to landward as: Coastal (First) ridge; Mex Abu Sir (Second) ridge; Gebel Maryut (Third) ridge and Khashm El Ish (Fourth) ridge.

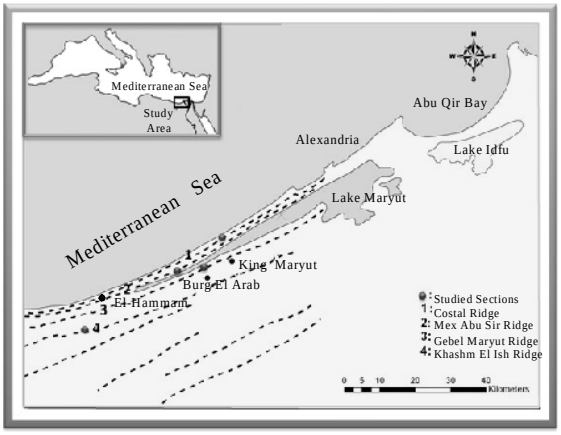

Fig. 1 Location map of the studied area showing the location of the limestone ridges (modified after [2])

M. A. Rashed and A. S. Mansour are with Geology Department, Faculty of Science, University of Alexandria, Alexandria, Egypt (e-mail: rashedmohamed@yahoo.com, ah_sadek@hotmail.com).

H. Faris and W. Afify are with Geology and Biology Department, Faculty of Education, University of Alexandria, Alexandria, Egypt.

II. Geological Setting

The study area represents a part of the Mediterranean coastal plain of the northwestern Egypt. It extends from west of Alexandria city southwestwards to near El Alamein, a distance of approximately 90 km. The coastal plain is covered by Quaternary deposits, which are represented by succession of several limestone ridges run parallel to the present shoreline and extend from Alexandria to Salum at Libyan border. These ridges are separated by elongate depressions covered by lagoonal, sabkha and alluvial deposits [1], [5]. The elevation of the ridges increases from the first coastal one (border the present coast with altitude of less than 10 m) to the most inland ridge (which is the highest and has altitude of about 100 m). At Burg El-Arab study area, only the first four ridges are well exposed. The coastal plain is bordered to the south by the outcropping vast tabular Middle Miocene Marmarica limestone plateau, which forms a tableland [13].

The rocks of the first (coastal) limestone ridge have snow white color and are characterized by low angle planar cross-stratification (Fig. 2 a). They are composed mainly of ooids, which are weakly cemented, well sorted and well rounded. The rocks of the second (Mex Abu Sir) ridge have creamy color and are characterized by tabular and trough cross-stratification (Fig. 2 b). Although the ooids are dominated, the rocks have less ooids and more bioclasts relative to the first ridge. Very thin calcrete crust occurs at the top of the ridge. Quarrying is active along this ridge.

The rocks of the third (Gebel Maryut) ridge are composed of creamy to light brown, fossils-rich limestone (Fig. 2 c). The elevation of this ridge is up to 35m above the Lake Maryut. The calcarenite sediments are interfingered and alternated with more than one thin horizon of loess sediments (geosoil), which are composed of carbonate grains mixed with quartz silt and clay minerals. Light brown, very hard and compacted calcrete layer is well developed on the top of the ridge. The calcarenite sediments overlie shallow marine to beach deposits including weakly cemented molluscan and foraminiferal limestones and beach boulders [5], [6]. The rocks of the fourth (Khashm El Ish) ridge, which is best exposed in the Khashm El Ish area, south to the El Hammam city, are composed of pink to brownish white, well cemented fossils- and intraclasts-rich limestones (Fig. 2 d). A soil profile with a well-developed caliche zone is developed on the top of the ridge with thickness reaches to 1.5m. The very hard and massive calcrete crust is underlain by partially cemented and nodular carbonate rocks. As a result of large-scale quarrying, this ridge is gradually disappearing.

III. Materials and Methods

A. Sampling

A total of 23 fresh and non-weathered carbonate block samples were collected along N-S profiles through the four ridges. The samples represent the different lithological varieties of the carbonate calcarenites. The rock samples are cored (of diameter 3.55cm) in three directions; normal, inclined and parallel to the bedding plane. A total of 85 carbonate core samples (69 dry and 16 saturated) are prepared and tested using the universal testing machine to document their geotechnical properties and declare the effect of diagenesis processes on the geotechnical properties (ultimate compressive strength, saturated compressive strength, softness coefficient, Young's modulus, anisotropy, unit weight, specific gravity, and porosity).

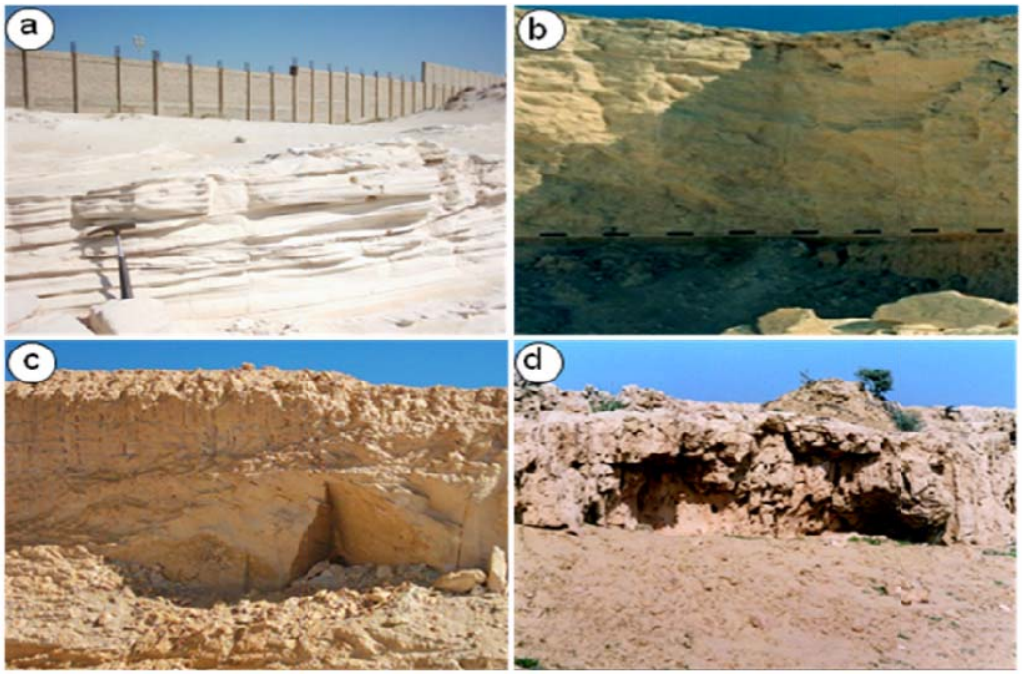

Fig. 2 Field Photographs showing the studied four limestone ridges a. the slightly cemented calcarenite first coastal ridge, b. the highly cemented second ridge, c. the more cemented third ridge and d. the highly weathered fourth ridge

B. Petrographical Studies

The petrography of the selected carbonate rock samples were examined and described morphologically, texturally and compositionally. A total of 50 thin sections were studied using the polarized microscope to determine the rock constituents and to describe the diagenetic features and the different porosity types. Few representative samples were selected for the Scanning Electron Microscopy work (SEM) to study the microfabrics. Representing thin sections were selected for point-counting to measure porosity. Bulk mineralogical composition of the carbonate rocks was determined by X-ray diffraction (XRD) using a Bruker AXS-XRD-Modal D8/Advance at X-ray Lab. of Chemistry Department in Texas A&M University. Standard reference curves and the d-values of the '104' diffraction peak were used to determine the Mg content as $MgCO_3$ (mol %) in calcite [14]. Calcite with less than 5 mol % $MgCO_3$ is considered low-Mg calcite (LMC) and that of 5-18 mol % $MgCO_3$ is referred to as high-Mg calcite (HMC). The relative weight percentages of aragonite and calcite were calculated using the ratio of the aragonite peak intensity to calcite peak intensity and applying the standard curve by [15].

C. Geotechnical studies

The cored samples were cleaned from dust and cutting remains using ultrasonic waves. The samples were placed in a conventional oven at 95^0 C and dried to a constant weight. The weight and dimensions of the core samples were measured using a sensitive balance and micrometer. The following geotechnical parameters have been measured and calculated:

Unit weight (γ): The unit weight of the plug samples was calculated by measuring the bulk volume and the weighed of the dry plugs.

$$\gamma = W_d/V_b \quad (1)$$

where, W_d is the dry weight (gm) and V_b is the bulk volume of the sample (cm^3). The unit weight is controlled by texture, mineral composition, diagenetic processes and geotectonic conditions of the area in which the rock exists [11], [16], [17].

Specific gravity (Gs): It is the weight of a unit volume of the solid phase of rocks excluding all voids. The pycknometer method described by [18] is used for measuring specific gravity.

Effective Porosity ($Ø_e$): It has been determined using the saturation method [19].

Total Porosity ($Ø_t$): It was calculated by applying the following equation:

$$Ø_t\ \% = (Gs\text{-}\gamma)/(Gs\text{-}\sigma_f)100 \quad (2)$$

where, Gs: Specific gravity, γ: unit weight, σ_f: density of the fluid filled the pores.

Ultimate compressive strength (UCS): It is the load per unit area at which a block fails by shear or splitting [20]. The unconfined compressive strength test is the most frequently used strength test for rocks. The studied rock samples were tested using the universal testing machine (Compressive Strength tester, Model ADR/BS2000–"ELE" England). The loading rate was 100 kg/cm^2/min. Well representative rock samples were selected and cored in three directions perpendicular, parallel and inclined on the bedding plane. The test was carried out following the standard test method for unconfined compressive strength of intact rock core specimen ASTM standard D 2938-95 [21] on 69 dry rock samples and 16 fully-saturated samples.

The compressive strength or (the stress) in the test specimen was calculated from the maximum compressive load on the specimen and the initial computed cross-sectional area as follows:

$$\sigma = P/A \quad (3)$$

where; σ = compressive strength, in (MPa), P = maximum load, and A = cross sectional area.

The compressive strength of the rocks is affected by internal and external factors. The former includes mineralogy, rock fabric, size and shape of grains, density, porosity, water content, temperature, and anisotropy. External factors are related to the test conditions including both specimen geometry and testing state (e.g. aspect ratio length/diameter (L/D), core ends, rate of coring, capping material and loading rate) [20]. The compressive strength also depends upon the orientation of load application with respect to microstructure (e.g. foliation in metamorphic rocks and bedding planes in sedimentary rocks). It was recommended that the aspect ratio (length/diameter) must be (2:1). Clearly it is not always possible to obtain a sufficient length of core for a 2:1 sample to be prepared. So the correction of compressive strength values with respect to the L/D ratio (L: Length and D: diameter) was calculated using the formula of [22], [23] as follows:

$$Co = Cp/(0.778 + 0.222D/L) \quad (4)$$

where, Co: is the compressive strength of the sample having a 1:1 L/D ratio, Cp: is the compressive strength of the same sample which have 2>L/D>1/3.

The Young's modulus (E): The modulus of elasticity was determined from the slope of the stress-strain curve [24]. It represents the stiffness of the material-resistance to elastic strain. As such, a stiffer material will have a higher elastic modulus. The general engineering classification chart for limestones and dolomites given by [25], which based on a plot of unconfined compressive strength against elastic modulus, has been used for classification of the studied coastal ridges. This classification provides a quantitative description in terms of two engineering characteristics, strength and deformation.

Softness Coefficient (K_P): The coefficient of softness for some saturated rock samples has been calculated using the formula of [16]:

$$K_P = R_{C\cdot w}/R_{C\cdot D} \quad (5)$$

where $R_{C.w}$: compressive strength of water saturated samples, $R_{C.D}$: compressive strength of dry samples.

Anisotropy: The strata orientation has a notable influence on the measured unconfined compressive strength of the rocks. The anisotropy of metamorphic and sedimentary rocks is mainly due to the presence of a single set of discontinuity surfaces such as cleavage, foliation, schistosity, joints, microfissuring or bedding. Sedimentary rocks can be isotropic or anisotropic depending on the spacing of bedding planes or lamina developed during deposition [26]. The variation of the measured compressive strength of the studied samples depend on the angles between the directions of the applied loads on the tested samples and the direction of the anisotropy (angle β) as summarized by [27]. The values of the compressive strength show two maxima, one when β = 0° (parallel to the bedding plane) and the other when β = 90° (perpendicular to the bedding plane), and a minimum when β is 45° (inclined on the bedding plane). The relative difference between the maximum and the minimum values differs from one rock type to the other depending on the degree of anisotropy of the material [28]. The concept of strength anisotropy in rocks, due to the effect of a single plane of weakness was originally developed by [29], who suggested the U-type relationship. Further investigations were conducted on the strength behavior of shale and slate by [30].

The degree of anisotropy of some selected rock samples of the studied four ridges was calculated using the "Anisotropy ratio" suggested by [31], and which is the ratio between the maximum compressive strength obtained at β=90° and the minimum compressive strength.

IV. Depositional and Diagenetic Fabrics

The petrographic study reveals that the carbonate rocks of the four coastal ridges have four main microfacies, which are ooid-grainstone (Fig. 3 a, b), bioclasts-ooid grainstone (Fig. 3 c, d), bioclastic grainstone (Fig. 3 e, f), and bioclasts-intraclast grainstone to packstone (Fig. 3 g, h), representing the first, second, third, fourth ridges, respectively. The rocks of the four ridges show progressive textural, mineralogical, and diagenetic alterations when tracing from the first to the fourth ridge. These changes are resulted from increasing duration in the meteoric water environment. The XRD analysis reveals that the most common carbonate minerals are aragonite and calcite. The calcite is represented by high Mg-calcite (HMC) and low Mg-calcite (LMC). Minor amount of dolomite and quartz are also detected in the third and fourth ridges. There is a gradual decrease in the content of aragonite and high Mg-calcite from the younger coastal ridge to the older fourth ridge, whereas the stable low Mg-calcite increases. The aragonite content ranges from 60 to 92% in the first ridge, from 25 to 48% in the second ridge, from 17 to 32% in the third ridge, and from 5 to10% in the fourth ridge, whereas the calcite content ranges from 10 to 40%, 45 to 70%, 60 to 75% and more than 75% in the four ridges, respectively. This mineralogical variation is attributed to the difference in the allochemical constituents, which are dominated by aragonitic ooids in the youngest ridges and calcitic bioclasts and intraclasts in the oldest ridges and the progressive meteoric diagenesis from the youngest to the oldest ridges including: the dissolution of some aragonitic components, stabilization of some aragonitic and high Mg-calcite components to more stable low Mg-calcite, and the increasing of precipitation of low Mg-calcite cement.

Four stages of meteoric water diagenesis have been recognized. The first stage "early cementation stage" marked the first ridge rock samples. The sediments in this stage are poorly cemented by little vadose cements, and have high percent of porosity (32-41%). The most common type of porosity observed is primary intergranular porosity (Fig. 3 a, b). The second stage "dissolution and cement precipitation stage" characterizes the rocks of the second ridge. The sediments are more affected by meteoric diagenesis and characterized by more cementation and more dissolution of the aragonitic ooids. The oomoldic porosity (18-32%) is the most common type of porosity observed (Fig. 3 c, d). The third stage "dissolution, cementation, and recrystallization stage" characterizes the rocks of the third ridge. The sediments are poor to well cemented with variable percent of porosity (10-35%) of primary intergranular porosity (Fig. 3 e), besides secondary moldic and vuggy porosity (Fig. 3 f). The final stage "micritization, calcretization and compaction stage" that marked the fourth ridge rock samples, at which the sediments have undergone more diagenetic effects including, highly cementation by different types of cements, which reduced the porosity (3-23%), micritization and formation of calcrete layer.

V. Results and Discussion

A. Unit Weight and Porosity

The *unit weight* (γ) of the studied samples ranges between 1.71 and 1.98 g/cm^3 (av. 1.85 g/cm^3, Table I) for the first ridge, between 2.19 and 1.87 g/cm^3 (av. 2.01 g/cm^3) for the second ridge, between 2.48 and 1.81 g/cm^3 (av. 2.10 g/cm^3) for the third ridge, and between 2.54 and 2.00 g/cm^3 (av. 2.26 g/cm^3) for the fourth ridge. There is a general increase in the measured unit weight values from the first to the fourth ridges. The low values of the first ridge samples are accompanied with high porosity and low cementation of the rocks, where the sediments of the older ridges are more affected by subaerial diagenetic processes and more cemented than those of the first ridge.

The *specific gravity* (Gs) of the studied samples ranges between 2.89 and 2.93 g/cm^3 (av. 2.91g/cm^3) for the first ridge, between 2.82 and 2.69 g/cm^3 (av. 2.74 g/cm^3) for the second ridge, between 2.84 and 2.73g/cm^3 (av. 2.78 g/cm^3), for the third ridge, and between 2.80 and 2.70 g/cm^3 (av. 2.77 g/cm^3) for the fourth ridge. The values of the first ridge resemble the value of specific gravity of aragonite (2.90 g/cm^3), whereas the values of the other ridges close to the specific gravity of calcite (2.70 g/cm^3) [32]. This agrees with the predominance of aragonite in the limestone of the first

ridge and the increasing of calcite on the expense of aragonite in the older ridges as detected by the mineralogical analysis.

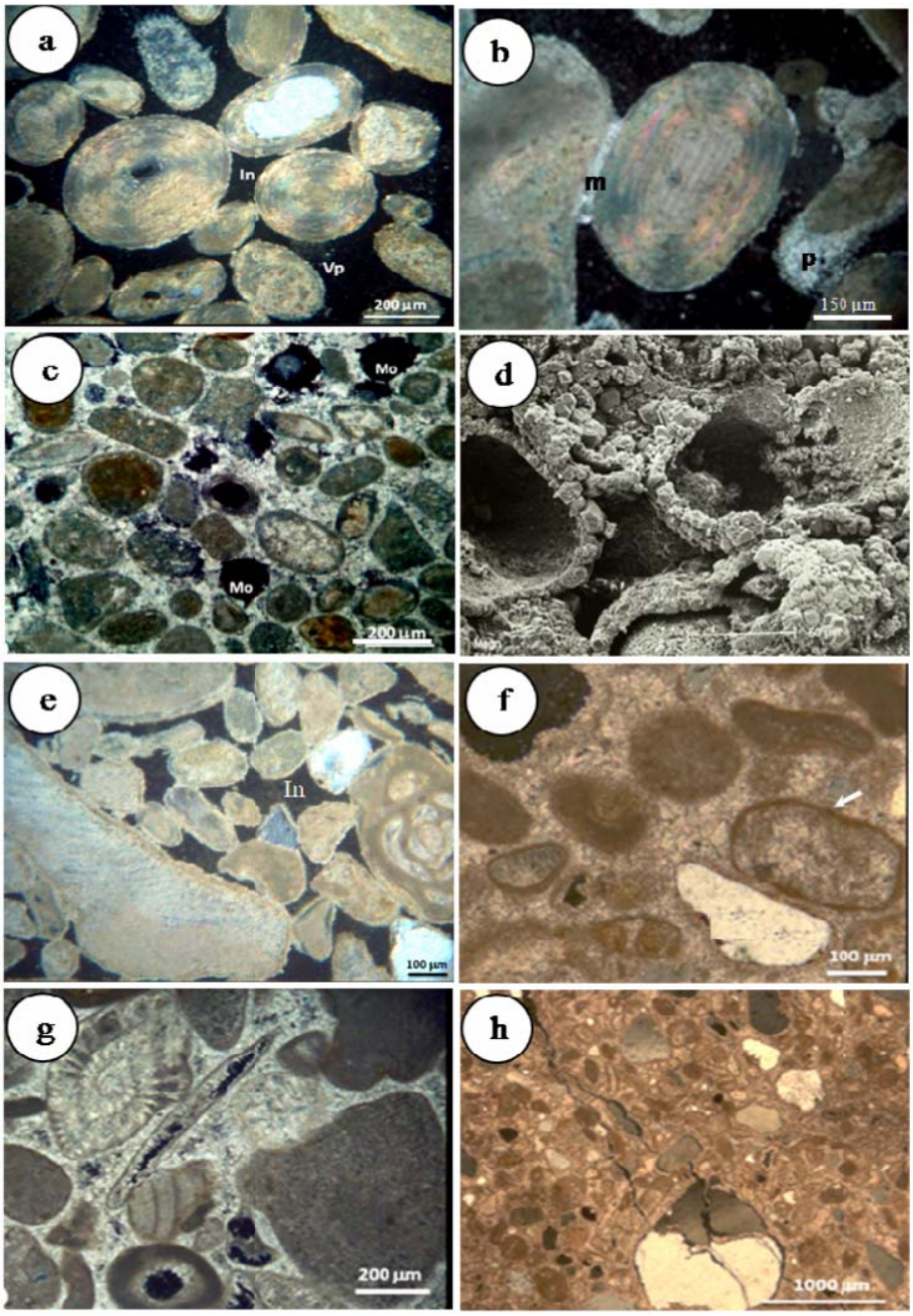

Fig. 3 Photomicrographs and SEM of the calcarenite limestones of the four ridges. The first ridge a & b: Note the dominance of ooids with high primary intergraunlar porosity (In), with little vadose cement (microcrystalline cement partially coated some ooids a, meniscus (m), pendant (p) at b. The second ridge c & d: The primary intergranular porosity has been reduced by sparry calcite cement. Oomoldic (Mo) and intragranular porosities are observed. d SEM micrograph shows the leaching of the ooids, leaving micrite envelopes and forming oomolds. The third ridge e & f: Note the dominance of bioclasts and lithoclasts with the variation of porosity from very low to high with different types, and reduced by different fabrics of cements. The fourth ridge g & h: Note the highly cementation of the rock and the reduction of the porosity. Micritization of bioclasts and development of micritic envelopes are observed in the rocks of the last two ridges (arrow). Note the fracturing of the quartz grains as a result of some pressure h

TABLE I
SPECIFIC GRAVITY (GS), UNIT WEIGHT (Γ), TOTAL AND EFFECTIVE POROSITY ($Ø_T$ AND $Ø_E$) OF THE FOUR RIDGE ROCK SAMPLES

	First Ridge					Second Ridge					Third Ridge					Fourth Ridge				
	S.No	γ g/cm³	Gs g/cm³	Øt %	Øe %	S.No	γ g/cm³	Gs g/cm³	Øt %	Øe %	S.No	γ g/cm³	Gs g/cm³	Øt %	Øe %	S. No	γ g/cm³	Gs g/cm³	Øt %	Øe %
Vertical direction	1	1.98	2.93	32.42	22.98	1	1.90	2.71	29.89	27.11	1	1.90	2.84	33.10	31.33	1	2.32	2.79	16.85	15.53
	2	1.89	2.91	35.05	24.72	3	1.92	2.75	30.18	26.46	2	2.47	2.80	11.79	9.47	2	2.54	2.80	9.29	7.45
	4	1.71	2.90	41.03	31.73	4	2.09	2.69	22.30	21.47	3	2.00	2.78	28.06	24.63	4	2.24	2.79	19.71	19.49
	5	1.78	2.91	38.83	27.98	5	1.99	2.70	26.30	24.83	4	2.46	2.75	10.55	3.66	6	2.31	2.80	17.50	11.25
	10	1.83	2.89	36.68	25.67	6	1.94	2.72	28.68	26.65	5	2.16	2.73	20.88	16.39	7	2.23	2.70	17.41	12.79
	12	1.92	2.91	34.02	23.27	7	1.88	2.76	31.88	27.73	6	2.02	2.74	26.28	25.11	8	2.30	2.78	17.27	16.20
	14	1.94	2.91	33.33	23.07	8	1.94	2.78	30.22	24.97	7	1.99	2.78	28.42	26.78	12	2.14	2.79	23.30	22.80
						9	1.90	2.77	31.41	25.63	8	1.90	2.79	31.90	30.81	13	2.24	2.78	19.42	19.21
						10	1.88	2.73	31.14	26.36	9	2.05	2.77	25.99	23.09	14	2.42	2.72	11.03	7.68
						11	2.18	2.82	22.70	22.21										
	Min	**1.71**	**2.89**	**32.42**	**22.98**	**Max**	**2.18**	**2.82**	**31.88**	**27.73**	**Max**	**2.47**	**2.84**	**33.10**	**31.33**	**Max**	**2.54**	**2.80**	**23.30**	**22.80**
	Max	**1.98**	**2.93**	**41.03**	**31.73**	**Min**	**1.88**	**2.69**	**22.30**	**21.47**	**Min**	**1.90**	**2.73**	**10.55**	**3.66**	**Min**	**2.14**	**2.70**	**9.29**	**7.45**
	Av.	**1.86**	**2.91**	**35.91**	**25.63**	**Av.**	**1.96**	**2.74**	**28.47**	**25.34**	**Av.**	**2.11**	**2.78**	**24.11**	**21.25**	**Av.**	**2.30**	**2.77**	**16.86**	**14.71**
nclined direction	1	1.89	2.93	35.49	24.44	1	1.87	2.71	31.00	27.21	1	1.98	2.84	30.28	31.33	1	2.35	2.79	15.77	14.71
	2	1.84	2.91	36.77	25.43	3	2.13	2.75	22.55	22.08	2	2.45	2.80	12.50	9.47	2	2.32	2.80	17.14	14.09
	4	1.77	2.90	38.97	28.29	4	2.12	2.69	21.19	20.81	3	2.00	2.78	28.06	24.63	4	2.19	2.79	21.51	21.27
	5	1.79	2.91	38.49	27.21	5	1.96	2.70	27.41	24.99	4	2.48	2.75	9.82	3.66	6	2.39	2.80	14.64	13.38
	10	1.82	2.89	37.02	26.87	6	1.96	2.72	27.94	25.30	5	2.12	2.73	22.34	16.39	7	2.29	2.70	15.19	12.69
	12	1.86	2.91	36.08	25.20	7	1.97	2.76	28.62	25.92	6	1.97	2.74	28.10	25.11	8	2.16	2.78	22.30	21.27
	14	1.82	2.91	37.46	26.09	8	2.19	2.78	21.22	20.05	7	2.01	2.78	27.70	26.78	12	2.00	2.79	28.32	25.99
						9	2.10	2.77	24.19	21.55	8	1.81	2.79	35.13	30.81	13	2.12	2.78	23.74	20.55
						10	2.00	2.73	26.74	23.50	9	1.93	2.77	30.32	23.09	14	2.11	2.72	22.43	21.14
						11	2.06	2.82	26.95	22.75										
	Min	**1.77**	**2.89**	**35.49**	**24.44**	**Max**	**2.19**	**2.82**	**31.00**	**27.21**	**Max**	**2.48**	**2.84**	**35.13**	**31.33**	**Max**	**2.39**	**2.80**	**28.32**	**25.99**
	Max	**1.89**	**2.93**	**38.97**	**28.29**	**Min**	**1.87**	**2.69**	**21.19**	**20.05**	**Min**	**1.81**	**2.73**	**9.82**	**3.66**	**Min**	**2.00**	**2.70**	**14.64**	**12.69**
	Av.	**1.83**	**2.91**	**37.18**	**26.22**	**Av.**	**2.04**	**2.74**	**25.78**	**23.42**	**Av.**	**2.08**	**2.78**	**24.92**	**21.25**	**Av.**	**2.21**	**2.77**	**20.11**	**18.34**
parallel direction	1	1.97	2.93	32.76	23.11	1	2.08	2.71	23.25	23.28	1	1.84	2.84	35.21	31.33	1	2.34	2.79	16.13	15.54
	2	1.91	2.91	34.36	24.22	3	1.99	2.75	27.64	24.22	2	2.43	2.80	13.21	9.47	2	2.37	2.80	15.36	13.14
	4	1.72	2.90	40.69	30.43	4	2.11	2.69	21.56	20.91	3	1.99	2.78	28.42	24.63	4	2.39	2.79	14.34	12.60
	5	1.74	2.91	40.21	28.66	5	2.01	2.70	25.56	23.21	4	2.44	2.75	11.27	3.66	6	2.34	2.80	16.43	15.44
	10	1.80	2.89	37.72	27.63	6	2.04	2.72	25.00	23.86	5	2.19	2.73	19.78	16.39	7	2.27	2.70	15.93	14.59
	12	1.95	2.91	32.99	23.80	7	2.02	2.76	26.81	23.11	6	1.99	2.74	27.37	25.11	8	2.21	2.78	20.50	19.26
	14	1.94	2.91	33.33	24.07	8	2.15	2.78	22.66	20.75	7	1.98	2.78	28.78	26.78	12	2.03	2.79	27.24	26.85
						9	1.95	2.77	29.60	25.6	8	1.96	2.79	29.75	30.81	13	2.19	2.78	21.22	20.42
						10	1.90	2.73	30.40	25.72	9	2.01	2.77	27.44	23.09	14	2.21	2.72	18.75	17.73
						11	2.10	2.82	25.53	23.30										
	Max	**1.97**	**2.93**	**40.69**	**30.43**	**Max**	**2.15**	**2.82**	**30.40**	**25.72**	**Max**	**2.44**	**2.84**	**35.21**	**31.33**	**Max**	**2.39**	**2.80**	**27.24**	**26.85**
	Min	**1.72**	**2.89**	**32.76**	**23.11**	**Min**	**1.90**	**2.69**	**21.56**	**20.75**	**Min**	**1.84**	**2.73**	**11.27**	**3.66**	**Min**	**2.03**	**2.70**	**14.34**	**12.60**
	Av.	**1.86**	**2.91**	**36.01**	**25.99**	**Av.**	**2.04**	**2.74**	**25.80**	**23.40**	**Av.**	**2.09**	**2.78**	**24.58**	**21.25**	**Av.**	**2.26**	**2.77**	**18.43**	**17.29**
	Total Max	1.98	2.93	41.03	31.73	**Total Max**	**2.19**	**2.82**	**31.88**	**27.73**	**Total Max**	**2.48**	**2.84**	**35.21**	**31.33**	**Total Max**	**2.54**	**2.80**	**28.32**	**26.85**
	Total Min	1.71	2.89	32.42	22.98	**Total Min**	**1.87**	**2.69**	**21.19**	**20.05**	**Total Min**	**1.81**	**2.73**	**9.82**	**3.66**	**Total Min**	**2.00**	**2.70**	**9.29**	**7.45**
	Total Av.	1.85	2.91	36.47	26.12	**Total Av.**	**2.01**	**2.74**	**26.64**	**24.02**	**Total Av.**	**2.09**	**2.78**	**24.53**	**21.25**	**Total Av.**	**2.26**	**2.77**	**18.65**	**16.82**

The *total porosity* ($Ø_t$) values lie between 41.03 and 32.42% (av. 36.37%), between 31.88 and 21.19% (av. 26.64%), between 35.21 and 9.78% (av. 24.31%) and between 28.32% and 9.29% (av. 18.65%) for the four ridges, respectively (Table II). The *effective porosity* ($Ø_e$) values range between 31.73 and 22.98% (av. 25.95%), between 27.73 and 20.05%

(av. 24.05%), between 34.99 and 3.66% (av. 21.63%) and between 26.85 and 7.45% (16.78%) for the four ridges, respectively. The relatively high values of the porosity of the rocks of the first ridge are related to the textural and diagenetic characters. The sediments of this youngest ridge have not suffered diagenetic impact and are poorly cemented, besides, they have equi-dimensional, well sorted and loosely packed grains, without fine-grained matrix. Whereas, the rocks of the second ridge are more affected by subaerial diagenetic processes, more cemented and more packed, and thus, have relatively low porosity values. The wide range of the porosity of the third ridge samples is attributed to the variation in the grain size and degree of cementation of the sediments as a result of fluctuation of water table. The more porous layers, with mainly intergranular porosity (Fig. 3 e), are characterized by more coarse grains, high content of shell fragments and little cement. On the other hand, the high degree of cementation, micritization of the grains, formation of calcrete layers, and precipitation of micritic matrix, all of them, resulted in decreasing porosity of the rocks in other layers (Fig. 3 f). The fourth ridge rock samples have relatively the lowest values of porosity compared with the other ridges. The rocks show more progressive diagenetic alterations including more micritization, calcretization, cementation, and slightly compaction (Fig. 3 g, h).

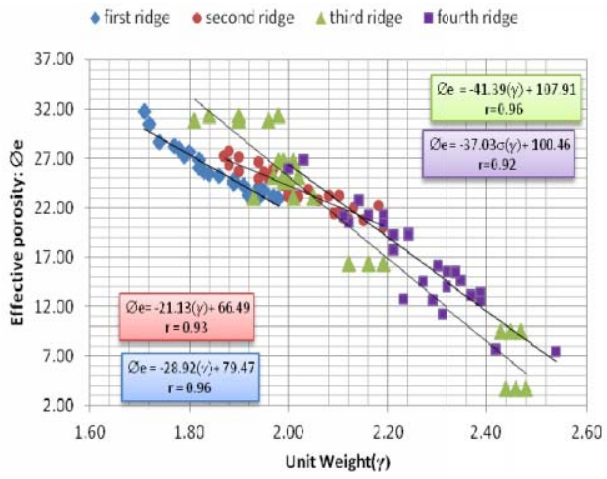

Fig. 4 The relationship between effective porosity ($Ø_e$) and the unit weight (γ) for the four ridges rock samples

The unit weight is inversely proportional related to the effective porosity with high correlation coefficient ($0.92 \leq r \leq 0.96$) for each ridge separately (Fig. 4), and (r = 0.86) for the four ridges together, indicating more or less homogeneity in pore network distribution. The following equations could be used to calculate the effective porosity values in terms of unit weight:

$$Ø_e = -28.92\gamma + 79.47 \ (r= 0.96), \text{ for the first ridge} \quad (6)$$

$$Ø_e = -21.13\gamma + 66.49 \ (r= 0.93), \text{ for the second ridge} \quad (7)$$

$$Ø_e = -41.39\gamma + 107.91 \ (r= 0.96), \text{ for the third ridge} \quad (8)$$

$$Ø_e = -37.03\gamma + 100.46 (r= 0.92), \text{ for the fourth ridge} \quad (9)$$

$$Ø_e = -29.96\gamma + 83.69 \ (r= 0.86), \text{ for the four ridges} \quad (10)$$

B. The Ultimate Unconfined Compressive Strength

The ultimate compressive strength (UCS) varies from 2.74 to 1.22 MPa (av. 1.94 MPa), from to 8.77 to 3.12 MPa (av. 5.36 MPa), from 71.31 to 1.29 MPa (av. 12.88 MPa), from 59.56 to 5.51MPa (av. 18.81 MPa) for the first, second, third, fourth ridges rock samples, respectively (Table II). The values of compressive strength of the samples of the first, second, and most of the third ridges lie within the range of weakly cemented carbonate rocks (0.3-12 MPa), whereas most of tested fourth ridge rock samples and few rock samples of the third ridge can be classified as highly cemented (12.5-100 MPa) according to classification of [33] for carbonate formations. In general, there is a marked increase in the compressive strength from the first to the fourth ridge, which is contributed to many factors including, the type and degree of cementation, grain fabric and mineralogy [17]. The strength of carbonate rocks generally increases over geologic time due to recrystallization, cementation and decreasing porosity. Geologically, the older carbonate rocks (the fourth ridge) tend to be stronger than the younger rocks (first ridge). The lowest values of (UCS) detected for the first ridge rock samples is related to the loosely packing, weakly cementation of the sediments, besides the irregularly distributed meniscus and pendent calcite cement (Fig. 3 a, b), which result in decreasing the ability of these rocks to withstand crushing under direct pressure. Although the rocks of the second ridge show relatively high degree of cementation, their (UCS) values are small relative to the fourth ridge. This may be attributed to the presence of oomoldic pores and the sparry nature of the low Mg-calcite cement in the second ridge (Fig. 3 c, d). It is well known that sparite imparts lower strength to the rock than micrite. These results agree with the observations of [20], that the higher the percent of isolated vugs in the oolitic carbonate rocks, the lower their compressive strength.

The third ridge rock samples show wide variation in their (UCS) values. This may be related to the heterogeneity in cement distribution and grain size [24]. Some samples have low values, resemble the first ridge samples. These low values are attributed to the high primary intergranular and biomold porosity resulted from dissolution of some shell fragments and low cementation, besides the abundance of thin shells with large internal cavities. These shells act as a plane of weakness and decrease the rock strength. Other samples have high values, resemble the fourth ridge samples. The high values are detected for the calcretized rocks, which are characterized by high degree of cementation, low porosity, presence of micrite matrix and minor amounts of more hard minerals (Quartz and dolomite), and the reduction in grain size [36].

Finally, it can be suggested that the variation of the (UCS) values of the Quaternary carbonate ridges depended on the porosity, crystal size, type of cements (micrite or sparite) and the nature of their distribution, amount of vugs and their size

distribution, age of carbonate rocks, and mineralogy. This agrees with many authors' observations [11], [17], [20], [34].

C.Ultimate Compressive Strength and Unit Weight, Total Porosity Relationships

A positive relationship between unit weight (γ) and compressive strength with correlation coefficient (r = 0.78) is shown in Fig. 5. The following equation could be used to calculate the ultimate compressive strength of the rocks of the Quaternary carbonate ridges in terms of their unit weight:

$$UCS = 15.00\gamma - 25.40 \ (r = 0.78) \quad (11)$$

A relatively high negative exponential relationship has been detected between total porosity and compressive strength (r = 0.80, Fig. 5). This plot reveals that with increasing the porosity of the rocks, its resistance against the stress will decrease, and the rock will fail at a smaller stress as a result of weakness of the rock frame. The following exponential equation could be used to calculate the ultimate compressive strength of the studied rocks in terms of their total porosity:

$$UCS = 29.22e^{-0.074\emptyset t} \ (r = 0.80) \quad (12)$$

D.Stress-Strain Relationships

The stress-strain curves and the load-deformation characteristics of the four ridges rock samples are shown in Fig. 6. The uniaxial stress strain curves have S-shape. The stress strain curves of the second, third, fourth ridges rock samples are of brittle rock type, because they have a straight linear elastic deformation with little strain and high stress. After maximum load, the stress-strain curve of the brittle carbonate rocks fall steeply with sudden fracture and little or no plastic deformation. On the other hand, the stress strain curves of the first and some of the third ridge samples may be considered as semi ductile rock samples. The rocks exhibit a gradual fall after the maximum load has been reached with little brittleness and relatively high ductility.

The increase in brittleness and decrease in plasticity of the stress strain curves form the first to the fourth ridges samples may attribute to several factors, the most important one is the porosity. The brittle strength increases with decreasing porosity. Reference [35] stated that the nonlinearity of the stress strain curve (e.g. the first ridge, and some of the third ridge samples) is usually attributed to that the material is undergoing a rearrangement of its internal microscopic structure (dislocation motion). Materials lacking this mobility, for instance by having internal microstructures that block dislocation motion, are usually brittle rather than ductile (e.g. the second, some of the third and the fourth ridges samples). In addition, as grains become small in size (e.g. the fourth ridge); the fracture becomes more brittle, where the dislocations have less space to move. Here, the dislocations cannot move very far before fracture, which leads to decreasing of plastic deformation and the material's fracture is more brittle.

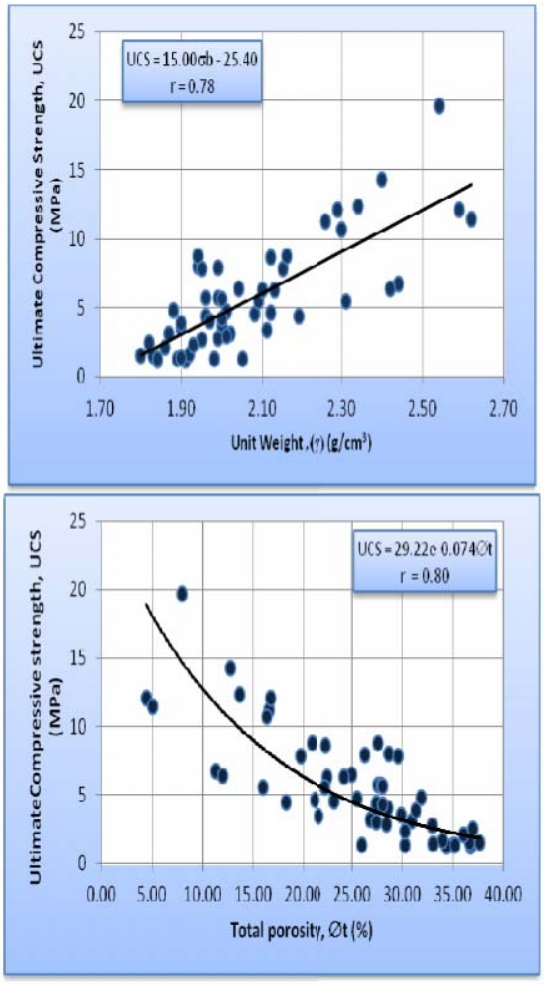

Fig. 5 Plotting the ultimate compressive strength (UCS) versus the unit weight (γ) and the total porosity ($\emptyset_t$) measured for the four carbonate ridges

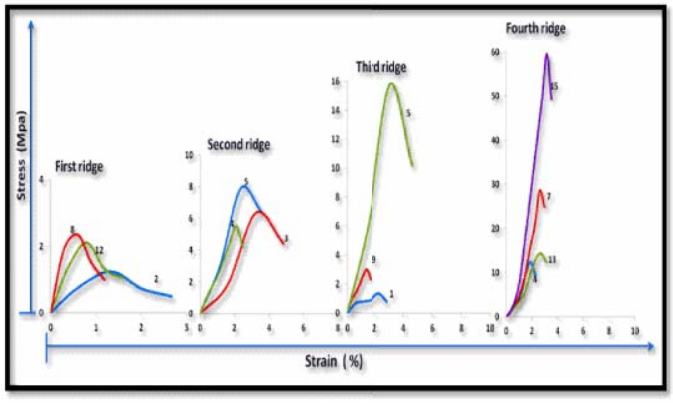

Fig. 6 Stress-strain curves for some representative rock samples from the studied carbonate four ridges

TABLE II
GEOTECHNICAL PROPERTIES OF THE FOUR RIDGES ROCK SAMPLES IN THREE DIRECTIONS. UCS, SUCS, E, KP ARE COMPRESSIVE STRENGTH, SATURATED COMPRESSIVE STRENGTH, YOUNG'S MODULUS AND SOFTNESS COEFFICIENT

		Vertical direction				Inclined direction				Parallel direction				
Ridge No.	**Sample No.**	**UCS_V**	**$SUCS_v$**	**E_v**	**Kp_V**	**UCS_I**	**$SUCS_I$**	**E_I**	**Kp_I**	**UCS_H**	**$SUCS_H$**	**E_H**	**Kp_H**	**Anisotropy ratio**
First ridge	2	1.29		1.46		1.24		1.25		1.22	0.37		0.30	1.06
	8	2.57		2.15		2.34		6.55		2.64		3.90		1.13
	10	2.46	1.32	1.70	0.54	1.52				1.51		1.53		1.63
	12	1.63				2.10	0.94	3.50	0.45	2.74	0.83	3.93	0.30	1.68
	max	2.57				2.34				2.74				
	min	1.29				1.24				1.22				
	Av.	1.99				1.80				2.03				1.38
Second ridge	1	3.53		4.29		3.12		4.03		4.52				1.45
	3	6.34		1.52		3.74		1.14		5.72		5.29		1.70
	4	5.51		2.71		4.63		1.62		3.41		2.94		1.62
	5	7.90		2.63		4.37	3.95	1.12	0.90	4.68		1.19		1.81
	6	8.0				5.72		4.35		6.44		3.27		1.40
	7	4.78		2.66		4.05				3.16				1.51
	8	8.77		2.13		4.41				7.82		3.79		1.99
	9	3.85	3.46		0.90	6.34	2.39		0.38	7.82	2.92	5.79	0.37	2.03
	max	8.77				6.34				7.82				
	min	3.53				3.12				3.16				
	Av.	6.09				4.55				5.45				1.69
Third ridge	1	1.40	0.57	2.30	0.41	1.29		1.64		1.32		1.14		1.09
	2	71.31	26.31	4.23	0.37	22.97		5.76		42.52	21.11	1.14	0.50	3.10
	3	5.62		2.81		4.26	2.16	3.36	0.51	2.81				2.00
	5	8.73	4.18	3.26	0.48	8.63		1.81		15.80		4.17		1.83
	9	1.32		1.19		2.31		2.26		2.97		3.26		2.25
	max	71.31				22.97				42.52				
	min	1.32				1.29				1.32				
	Av.	17.68				7.89				13.08				2.05
Fourth ridge	4	12.34		4.41		11.23		7.04		12.06		2.23		1.10
	7	28.06		5.14		11.43		5.43		19.65		6.44		2.45
	8	6.76	6.61		0.98	5.51				6.40		2.18		1.23
	13	14.24		4.51		10.71		7.07		12.06		7.38		1.33
	15	59.56		5.48		24.11	12.16		0.50	28.48		9.47		2.09
	51	35.56				13.41				34.25	30.87	3.60	0.90	2.65
	max	59.56				24.11				34.25				
	min	6.76				5.51				6.40				
	Av.	26.09				12.73				18.82				1.81

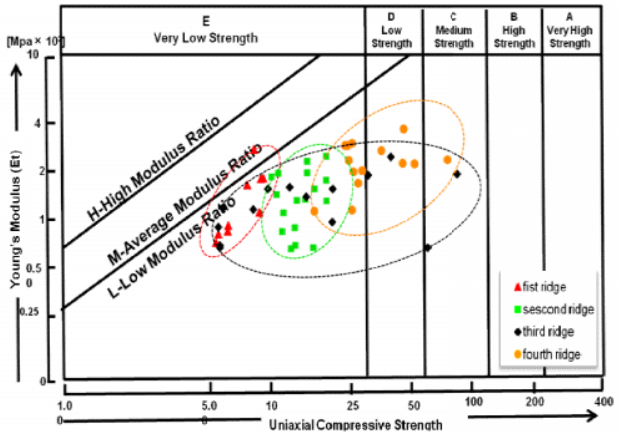

Fig. 7 Plotting uniaxial compressive strength against Young's modulus results of the studied rocks on Deere's chart

The modulus of elasticity (Young's modulus) ranges between 6.55 to 1.25 MPa (av. 2.89 MPa), 5.79 to 1.12 MPa (av. 2.97 MPa), 5.76 to 1.14 MPa (av. 2.74 MPa), 9.47 to 2.18 MPa (av. 5.39 MPa), for the first, second, third, and fourth ridges rock samples, respectively (Table II). Plotting of the Young's modulus values of the samples against their ultimate compressive strength in the general chart for engineering classification of limestone proposed by [25], is shown in Fig. 7. The plot reveals that most of the four ridges rock samples can be classified as very low strength (<28 MPa).

Some rock samples of the third and fourth ridges can be considered low (27-55 MPa) to medium strength (55-110 MPa). There is a general increase in the strength of the samples of the first ridge to those of the fourth ridges, whereas the samples of the third ridge show wide variation. All the studied rock samples have a low modulus ratio (EL).

E. Water Stability and Softness Coefficients (K_P)

The ultimate compressive strength and modulus of elasticity values are reduced significantly after saturation of the studied rock samples. Reference [37] believed that the pore water softens the bonding strength. The stone appears sound and dry, but wetting cause soften to such an extent that it may fall apart. The calculated softness coefficients (Kp) for some selected rock samples ranges between 0.30 and 0.54 (av. 0.41), 0.37 and 0.90 (av.0.64), 0.37 and 0.51 (av. 0.45), 0.81 and 0.98 (av. 0.89) for the first, second, third, and fourth ridges rock samples, respectively (Table II). The first and some of the third ridges rock samples show softness coefficients (Kp) higher than the rock samples of the other ridges, which is related to the high porosity and deficiency of cement (first ridge), in addition to the dissolution of some components (third ridge). As porosity increases, water is absorbed by the rocks in greater amount, which creates a higher pore water pressure and decrease the strength of the samples.

The difference between stress-strain curves for saturated and dry rock samples for each ridge is shown in Fig. 8. The post-peak stress-strain curve become flatter in case of the (UCS) tested on saturated samples for all ridges samples, with relatively lower strength, lower brittleness, and higher ductility. This may attribute to the increasing in fracture porosity after failure, which creates pore water pressure that enhances the rate of increase in strain.

F. Anisotropy

The strata orientation has a notable effect on the measured unconfined compressive strength. The rock will fail more easily if it contains discontinuities inclined to the direction of principal stress. The maximum compressive strength values have been recorded for some samples cored in the vertical and parallel directions with total averages 2.28, 6.71, 19.42, and 25.30 MPa for the four ridges rock samples, respectively. Meanwhile, the minimum compressive strength values have been recorded for most samples cored in the inclined direction with averages 1.68, 3.97, 7.40, and 13.69 MPa for the four ridges, respectively. The resulted compressive strength values suggest anisotropy ratios of 1.37, 1.69, 2.05, and 1.81 for the four ridges, respectively (Table II). Reference [26] assumed that the maximum recorded compressive strength can be controlled by the compressive strength of the intact material, whereas the minimum compressive strength is controlled by the shear strength of the discontinuity. The anisotropy ratio, which is the ratio between the maximum to the minimum compressive strength, can indirectly describe the ratio between compressive strength of the material and the shear strength of the discontinuity. Therefore, the anisotropy ratio increases with either the increase of the compressive strength of the intact material or decrease of the shear strength of the discontinuities and via versa. According to classification of anisotropy recorded by [31], the first, second, fourth ridges rock samples can be classified as low anisotropic rocks, whereas the rocks of the third ridge can be considered medium anisotropy. The lowest and highest anisotropy values have been recorded for the first and the third ridges rock samples, respectively (Table II). This may attributed to the relatively homogeneity and well sorted ooid grainstone of the first ridge rock samples, and the relatively heterogeneity in grain size distribution of the third ridge rock samples, besides the abundance of shell fragments and algal debris which may produce lines of weakness within the rock that result in variation in the strength measured in different directions with respect to the bedding plane.

The uniaxial compressive strength values of the four ridges were plotted against β angle (at 90°, 45°, and 0°), which represent the orientations (vertical, inclined, parallel) to the bedding plane. The variation in UCS with respect to inclination of bedding results in "U-shape" anisotropy curve (Fig. 9) with minimum compressive strength at the inclined direction and maximum values at the vertical and parallel directions. These results are consistent with the results of [30] for triaxial test on slates. Reference [36] concluded that the higher values of UCS in case of rock samples compressed perpendicular and parallel to the bedding plane may be attributed to the least shearing strength in these directions. In case of inclined direction, the bedding planes were oriented close to the plane of maximum shear stress and resulted in the lowering of UCS values.

Finally, we can summarize the measured data of the geotechnical parameters of the rocks of the four carbonate ridges in Fig. 10. There is a gradual increase in the unit weight from the first to the fourth ridge, which is combined with decrease in total and effective porosity. The decrease in porosity reflects an increasing in the compressive strength from the first to the fourth ridge. The mechanical anisotropy shows an increasing trend from the first to the fourth ridge. A relatively wide range of the mechanical anisotropy has detected for the third ridge rock samples, which might related to heterogeneity in grain and pore size distribution and degree of cementation.

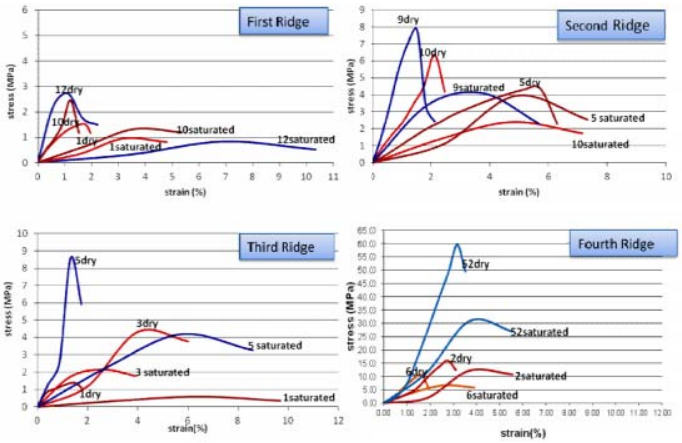

Fig. 8 Stress-strain curves for (UCS, SUCS) tested on representative dry and saturated rock samples of the four carbonate ridges

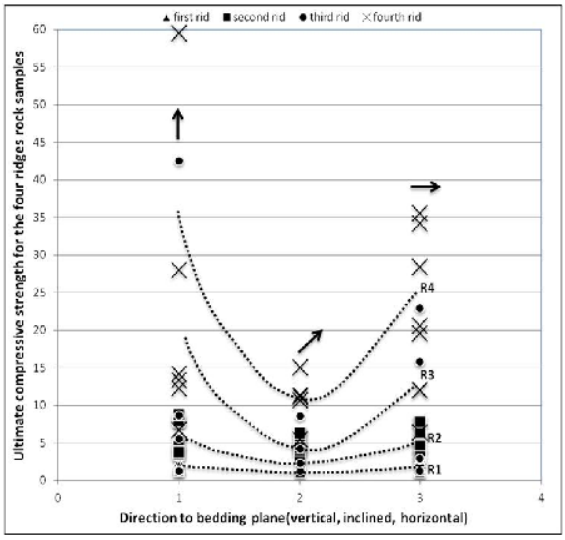

Fig. 9 Anisotropic behavior of compressive strength of the four ridges (R1, R2, R3, R4), respectively. 1, 2, 3 represents the (UCS) values measured in vertical, inclined, and parallel directions to the bedding plane

G.Mutual Relationships between Geotechnical Parameter: Correlation Matrix

The correlation matrix has been used to determine all possible simple correlation coefficient among some measured geotechnical parameters (Table III). Relatively strong negative and positive relationships have detected between different geotechnical parameters, with correlation coefficients ranges between ($0.7 \leq r \leq 0.9$), indicating a good linear relationships between the two measured variables. Few of the observed relationships are relatively weak ($0.04 \leq r \leq 0.30$).

H.Multiple Regression Analysis

Multiple regression analysis has been applied on some measured geotechnical parameters in order to evaluate the effect of two or more independent variables on a single dependent variable. The compressive strength has been selected as dependent variable throughout the analysis. Different geotechnical parameters have been selected as independent variables (Table IV).

A model has been determined to examine the relationship between log ultimate compressive strength (log UCS) as dependent variable and log effective porosity (log $Ø_e$), log unit weight (log γ), log specific gravity (log Gs) as independent variables. The log UCS is positively correlated with the log (γ) and negatively correlated with the log Øe and log Gs. From the multiple regression analysis, the values of the multiple coefficients of correlation (R), the coefficient of multiple determinations (R2), and the adjusted coefficient of multiple determinations (adjusted R2) are 0.78035, 0.60894, and 0.58680, respectively. The value of R2 relatively high, which indicate a strong association between the set of independent variables (logØe, log γ, log Gs) and the dependent variable (log UCS). The ANOVA table which assesses the overall significance of our model, as the value of F is higher than the value of F-significance, our model is significant. The values (p) and (t) give a rough indication of the impact of each predictor variable. A big absolute value t statistic (which is the coefficient divided by its standard error) and a small value of p ($p < 0.05$) suggest that a predictor variable is having a large impact on the criterion variable [37]. As a result we can use the derived model for the estimation of (UCS) as follows:

$$\log UCS = 3.572 + 3.113 \log \gamma - 4.749 \log Gs - 1.331 \log Ø_e \quad (13)$$

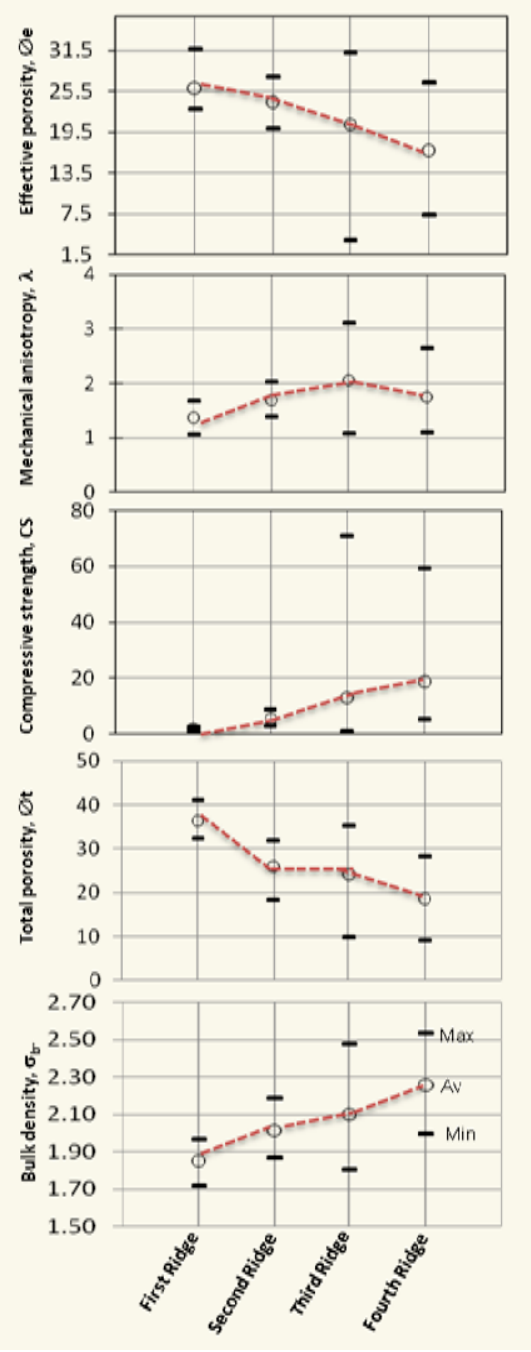

Fig. 10 Variation of the geotechnical properties through the studied four carbonate ridges

TABLE III
A CORRELATION MATRIX BETWEEN DIFFERENT GEOTECHNICAL PARAMETERS OF CARBONATE ROCKS OF THE FOUR COASTAL RIDGES *: STATISTICALLY SIGNIFICANT

	log UcsV	log UcsI	log UcsH	log av. γ	log av.Gs	log av.Øt	log av.Øe
log UcsV	1						
log UcsI	0.949*	1					
log UcsH	0.928*	0.958*	1				
log av.γ	0.863*	0.872*	0.878*	1			
log av.Gs	-0.275	-0.288	-0.266	-0.261	1		
log av.Øt	-0.822*	-0.802*	-0.841*	-0.950*	0.178	1	
log av.Øe	-0.724*	-0.677*	-0.776*	-0.781*	-0.040	0.872*	1

TABLE IV
MULTIPLE REGRESSION ANALYSIS FOR THE DEPENDENT VARIABLE (LOG UCS), AND INDEPENDENT VARIABLES (LOG ØE, LOG γ LOG GS) OF THE ROCKS OF THE FOUR RIDGES

Regression Statistics					
Multiple R	0.780345591				
R2	0.608939242				
Adjusted R2	0.586803727				
Standard Error	0.217637664				
Observations	57				
ANOVA					
	df	*SS*	*MS*	*F*	*Significance F*
Regression	3	3.9090723	1.3030241	27.509604	7.276x10-11
Residual	53	2.5104061	0.0473662		
Total	56	6.4194784			
	Coefficients	Standard Error	t Stat	P-value	
Intercept	3.572437486	2.1708823	1.6456155	0.1057614	
Log γ	3.113229782	1.6465221	1.8907914	0.0641241	
Log Gs	-4.74908657	2.5523384	-1.8606806	0.0683409	
Log Øe	-1.33113534	0.7094431	-1.8763101	0.0661237	

VI. SUMMARY AND CONCLUSIONS

Both the depositional texture and diagenesis of the calcarenite carbonate rocks of the most northern four Quaternary ridges in Egypt affect the different geotechnical properties of these rocks.

The petrographic study revealed that the carbonate rocks have four main microfacies, which are ooid-grainstone, bioclasts-ooid grainstone, bioclastic grainstone, and bioclasts-intraclast grainstone to packstone, representing the first, second, third, fourth ridges, respectively. The four ridges show progressive textural, mineralogical and mechanical changes when tracing from the first to the fourth ridge. The most common features of the diagenetic processes are the filling the intergranular porosity by sparry calcite, formation of oomoldic and vuggy porosity, micritization and calcretization. A gradual decrease in the aragonite content relative to low Mg- calcite is noticed as a result of the variation in carbonate grains types (ooids to bioclasts and lithoclasts); dissolution and/or stabilization of some aragonitic components to low Mg-calcite, and precipitation of calcite cement.

The geotechnical studies revealed that there is a decreasing in the values of the specific gravity from the rocks of the first to the fourth ridges, which is consistent with the variation in mineralogy from aragonite to calcite. Also, there is a general increase in the unit weight from the first to the fourth ridges, which is combined with decrease in total and effective porosity, and increase in cement precipitation. Equations (6)-(10) can be used for determining effective porosity in terms of the unit weight for the rocks of the four ridges.

The older carbonate rocks of the third and fourth ridges tend to be stronger and have higher values of the ultimate compressive strength than the rocks of the younger ridges. The (UCS) values of the first, second, and most of the third ridges samples lies within the range of weakly cemented carbonate rocks, whereas most of the fourth ridge and some of the third ridge rock samples can be classified as highly cemented. The (UCS) values of the carbonate ridges are directly proportional to the measured unit weight and have a negative exponential relationship with total porosity. Equations (11) and (12) can be used to obtain (UCS) of the four carbonate ridges in terms of their unit weight (γ), and total porosity ($Ø_t$).

The stress-strain curves of the four carbonate ridges are of S-shape with brittle behavior for the second, third, fourth ridges rock samples, whereas the curves of the first and some of the third ridges rock samples are of semi ductile type. The ductility of the rocks may attribute to the increase in grain size and porosity. The studied rocks can be classified as very low to medium strength and have a low modulus ratio. Also, the softness coefficient values of the first and some of the third ridges rock samples are relatively high. This may relate to the high porosity and deficiency of cement (first ridge); in addition to abundance of shell fragments with large intraparticle pore space (third ridge). This causes the increase of water absorption by rocks and creating a high porewater pressure and decreasing the strength of these samples.

The strata orientation have a notable effect on the measured (UCS), that the lowest values have been recorded for the samples cored in the inclined direction, whereas the highest values have been noticed in most samples cored in the vertical and parallel directions. In case of inclined direction, the bedding planes were oriented close to the plane of maximum shear stress.

The rocks of the first, second and fourth ridges can be classified as low anisotropic rocks, whereas the rocks of the third ridge can be considered medium anisotropy. The lowest and highest anisotropy values have been recorded for the first and the third ridges rock samples, respectively, which may attributed to the relatively homogeneity and well sorted grainstone of the rocks of the first ridge, and relatively heterogeneity in grain size distribution of the third ridge rock samples, besides, the abundance of shell fragments and algal debris. This may produce lines of weakness within the rock that result in variation in the strength measured in different directions with respect to the bedding plane.

REFERENCES

[1] N. M. Shukri, G. Philip, and R. Said, "The Geology of the Mediterranean Coast between Rosetta and Bardia, Part II: Pleistocene Sediments- Geomorphology and Microfacies," *Bull. Inst. Desert, Egypt*, vol. 37, pp. 395-433, 1956.

[2] K. W. Butzer, "On the Pleistocene Shore Lines of Arabs Gulf, Egypt," *Sed. Petrol. J.*, vol. 68, pp 626-637, 1960.

[3] M. M. El-Shazly, A. A. Shata, and I. M. Farag, "Lithology of the Neogene and Post-Neogene Sediments in Mersa Matruh area," *Geol. J. Egypt*, vol. 8, pp. 21-45, 1964.

[4] A. A. Selim, Origin and Lithification of the Pleistocene Carbonates of the Salum Area, Western Coastal Plain of Egypt," *Sed. Petrol. J.*, vol. 44, pp. 70-78, 1974.

[5] A. H. Hassouba, "Quaternary Sediments from the Coastal Plain of Northwestern Egypt (from Alexandria to El Omayid)," *Carb. and Evap*., vol. 10, pp. 8-44, 1995.

[6] H. M. El Asmar, H.M., "Recognition of Diagenetic Environments of the Pleistocene Carbonate Rocks at El Hammam, NW Mediterranean Coast of Egypt Using Stable Isotopes and Electron Microprobe," *N. Jb. Geol. Palaont. Mh*., vol. 1, pp. 7-22, 1994.

[7] H. M. Holail, "Diagenetic Trends of the Pleistocene Calcareous Ridges, Mersa Matruh area, Egypt," *Chem. Geol*., vol.106, pp. 375-388, 1993.

[8] A. El-Shahat, "Quaternary Dune Carbonates from the Mediterranean Coast of Egypt: Petrography and Diagenesis," *Env. Sci. J. Mansoura Univ. Egypt*, vol. 9, pp. 1-27, 1995.

[9] A. S. Mansour, "Sedimentological and Paleoenvironmental Studies of the Subsurface Miocene – Pliestocene Sequence at El-Dabaa, North Western Desert, Egypt," Unpublished Ph.D. Thesis, Fac. Sci., Alex. Univ., Egypt.

[10] M. I. Sayed Ahmed, O. Hegab, A. El-Shahat, and M. A. El-Hefnawi, "Strength properties for some Quaternary calcretes from the Northern Western Coastal Plain of Egypt," Zeit. Geol., Wissen, Berlin, vol 14, pp. 285–296, 1986.

[11] K. N. Sediek, and M. A. Rashed, M.A., "Petrography and Diagenetic Influence on the Petrophysical Characteristic of Quaternary Calcarenite North Western Desert, Egypt," *Eng. Geol. Hydrogeol. J*., pp. 127-151, 2004.

[12] A. A. Zahran, Geotechnical Study of Carbonate Rocks on the Area between Alexandria and El-Alamein along the Mediterranean Sea Coast of Egypt," *Assuit Unv. Bull. Env. Research.,* vol. 11, no. 1, pp. 35-46, 2008.

[13] R. Said, *The geology of Egypt*. Amesterdam, New York: Elsevier, 1962.

[14] D. N. Lumsden, "Discrepancy between Thin Section and X-Ray Estimates of Dolomite in Limestone," Sediment. Petrol. J., vol. 49, pp. 429-436, 1979.

[15] J. D. Milliman, *Marine Carbonates*. New York: Springer-Verlag, 1974.

[16] V. D. Lamatadze, *Engineering Geology. Engineering Petrology* (In Russian). Nedra, Leningrade, 1984.

[17] F. G. Bell, *Engineering Geology*. Blackwell Sci. Publ., 1993.

[18] N. V. Dakhanova, "Laboratory Work of Petrophysics (in Russian)," *Nedra, Moscow*, pp. 13-45, 1982.

[19] J. Koithara, K. Hashmy, and Y. M. Mehra, "The Laboratory Study of Core Samples from Productive Sandstones (Barails) in Rudrasafar field for Establishing Relationships between Electrical and Reservoir Parameters," Unpublished Report of the Institute of Petroleum Exploration, OWGC, 1968.

[20] B. K. Moh'd, "Compressive Strength of Vuggy Oolitic Limestones as a Function of Their Porosity and Sound Propagation," *Jordan J. Earth Env. Sci*., vol. 2, no. 1, pp. 18-23, 2009.

[21] ASTM, American Society for Testing and Materials, *Standard Test Method for Unconfined Compressive Strength of Intact Rock Core Specimens*. Test Designation D2938, Annual book of ASTM standards, Philadelphia, vol. 14, no. 2, 1995.

[22] L. Obert, and W. I. Duvall, *Rock Mechanics and the Design of Structures in rock*. New York, London, Sydney: John Wiley and Sons, 1967.

[23] R. C. Zaiangarov, P. E. Root, and S. D. Filimonov, *Practical Soil Mechanics* (In Russian). Moscow: Moscow State Univ. Publ., 1984.

[24] B. L. Overfield, "A Classification of Lower Paleozoic Carbonate-Bearing Rocks for Geotechnical Application," Unpublished M.Sc., Kentucky Univ., Kentucky, USA.

[25] D. U. Deere, "Geological Consideration," in: *Rock Mechanics in Engineering Practice*, K. G. Stagg, and O. C. Zeinkiewicz, Ed. New York, London, Sydney: John Wiley and Sons, 1968, pp.1-20.

[26] A. A. Al- Harthi, "Effect of Planar Structures on the Anisotropy of Ranyah Sandstone, Saudi Arabia," *Eng. Geol*., vol. 50, no. 1–2, pp. 49–57, 1998.

[27] T. Ramamurthy, R. G. Venkatappa, and J. Singh, "Engineering Behavior of phyllite," *Eng. Geol*., vol. 33, pp. 209–225, 1993.

[28] E. Hoek, and E. T. Brown, *Underground Excavations in Rock*. Instit. Mining and Metallurgy, London, 1980.

[29] J. C. Jager, "Shear Failure of Anisotropic rocks," *Geol. Mag*., vol. 97, pp. 65–72, 1960.

[30] E. T. Brown, L. R. Richards, and M. V. Barr, M.V., "Shear Strength Characteristics of Delabole Slates" in 1977 *Proc. Rock Engineers, Conf.*, Newcastle, pp. 31–51.

[31] J. Singh, T. Ramamurth, and G. V. Rao. G., "Strength Anisotropies in Rocks," Indian. Geotech. J., vol. 19, no. 2, pp. 147–166, 1989.

[32] J. A. Mandarino, and M. Fleischer, M., *Glossary of Mineral Species*. Tucson: Mineralogical Record Inc., 1991.

[33] A. R. Clark, and B.F. Walker, "A Proposed Scheme for the Classification and Nomenclature for Use in the Engineering Description of Middle Eastern Sedimentary Rocks," *Geotechnique*, vol. 27, pp. 93-99, 1977.

[34] M. A. Rashed, and K. N. Sediek, K.N., "Petrography, Diagenesis and Geotechnical Properties of El Rufuf Formation, Kharga Oasis," Egypt *African Earth Sci. J*., vol. 2, pp. 407- 423, 1997.

[35] T. H. Courtney, *Mechanical Behavior of Materials*, McGraw-Hill Series in Material Sci. and Eng., New York, 1990.

[36] R. K. Dubey, and V. K. Gairola, "Influence of Structural Anisotropy on Creep of Rocksalt from Simla Himalaya, India: An Experimental Approach," *Struct. Geol. J*., vol. 30, no. 6, pp. 710-718, 2008.

[37] N. Brace, et al., *SPSS for Psychologists: A Guide to Data Analysis Using SPSS for Windows, Versions 9, 10 and 11*. Lawrence Erlbaum Assoc., 2003.